Meddy–Seamount Interactions: Implications for the Mediterranean Salt Tongue

GUOHUI WANG AND WILLIAM K. DEWAR

Department of Oceanography, The Florida State University, Tallahassee, Florida

(Manuscript received 1 July 2002, in final form 6 May 2003)

ABSTRACT

A quasigeostrophic point vortex numerical model is used to explore interactions of eddies and seamounts. The ultimate objective of this study is to assess the role of meddy–seamount interaction as an input to Mediterranean salt tongue maintenance. Secondary objectives are to clarify the dynamics of meddy–seamount interaction. The results suggest that meddies survive seamount collisions with 60%–70% of their initial cores remaining intact as coherent vortices. Given observed formation rates, it appears meddies, in their interactions with seamounts, inject between one-quarter and one-half of the salt anomaly necessary to sustain the Mediterranean salt tongue. Other considerations suggest the anomalous mass flux by meddies is comparable to that due to the mean flow. In summary, meddies are important to the maintenance of the salt tongue, although other mechanisms are needed. Coherent vortex transport, of which meddies are one example, is a mesoscale process not well described by the downgradient mixing algorithms normally employed in general circulation models. More sophisticated mesoscale models are thus suggested by this study. In particular, survival by meddies of collisions with seamounts emerges as a potentially important limiting effect on the Mediterranean salt tongue. This effect has climatically significant implications for ocean simulations.

1. Introduction

Observations show that oceanic coherent vortices survive for years and migrate thousands of kilometers (Ebbesmeyer et al. 1986). Such vortices are also formed near oceanic fronts and thus possess cores with different properties than their host waters. Coherent vortices have thus been suggested as being important to the transport of ocean properties, heat and salt being two examples. To quantify this idea requires an understanding of vortex decay. ''Meddies,'' eddies containing water of Mediterranean origin, are a particularly well observed family of coherent vortices characterized by large salt and heat anomalies relative to their North Atlantic host environment. Richardson and Tychensky (1998) argue from float data that meddy–seamount interaction is a frequent occurrence and a potentially important meddy destruction mechanism. Such interactions might thus be significant to the maintenance of the Mediterranean salt tongue, perhaps the most important tracer signal in the World Ocean. The objective of this study is to numerically examine vortex–seamount interactions to assess their impacts on meddy life history and Mediterranean salt tongue maintenance.

Corresponding author address: Dr. Guohui Wang, Department of Oceanography, The Florida State University, Tallahassee, FL 32309-4320.
E-mail: gwang@ocean.fsu.edu

a. Background

It is now widely accepted that the ocean displays energetic variability. In addition to a variety of waves, the eddy field also involves several types of ''coherent vortices.'' These are, loosely speaking, long-lived eddies of nearly permanent form. An important category of the coherent vortex ''zoo'' are submesoscale coherent vortices (SCVs; McWilliams 1985), now thought to be fairly common. The Polymode Experiment in particular supported the ubiquity of submesoscale coherent vortices, culminating in Ebbesmeyer et al.'s (1986) estimate that there are 10 000 SCVs in the North Atlantic at any one time.

The conservative nature of many ocean tracers permits the formation regions of observed vortices to be deduced. The interesting result has thus emerged that coherent vortices can survive for years and move thousands of kilometers. These properties have led to the suggestion that coherent vortices constitute a principal means by which ocean tracers are transported. In such a scenario, mean state tracer gradients are controlled by vortex dissipation or destruction processes. A notable ramification of this hypothesis is that such transport differs significantly from that in downgradient (Fickian) diffusive parameterizations. These parameterizations, in use by essentially all modern large-scale numerical general ocean circulation models, connect mean tracer fields and mesoscale tracer transport. In contrast, coherent vortex transport is at most loosely constrained by mean tracer gradients; other distinctions are discussed by

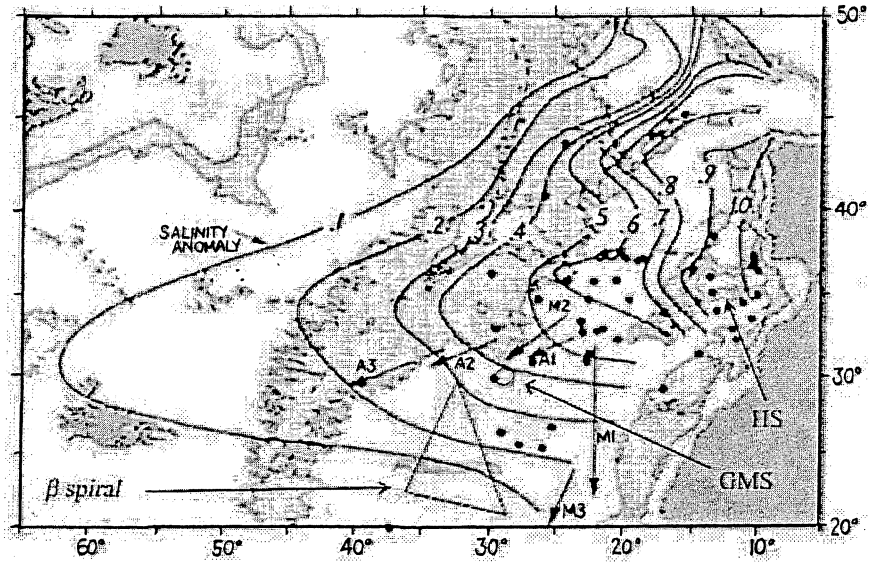

FIG. 1. Salinity anomaly in the North Atlantic is contoured (CI = 0.1 psu). The Mediterranean salt tongue appears as a westward-reaching zone of high salinity anomaly connected on the east to the Strait of Gibraltar. Also shown are the locations of the β spiral experiment, the Horseshoe Seamounts (HS), and the Great Meteor Seamounts (GMS). Observed locations of meddies appear as dots along with estimates of their propagation direction.

Pierrehumbert (1991). If coherent vortices are a dominant transport mechanism, numerical tracer transport models would be subject to revision.

b. Observations of meddies

Of all SCVs, perhaps the mostly widely recognized and frequently observed are the eddies of Mediterranean origin (i.e., meddies). The first meddy observation is usually credited to McDowell and Rossby (1978), although that interpretation is controversial (Prater and Rossby 1999). Most meddy observations come from the area of the Mediterranean salt tongue, shown in Fig. 1. Also appearing there are the locations of the β-spiral experiment (Armi and Stommel 1983), the Horseshoe Seamounts, and the Great Meteor Seamounts.

According to a recent review by Richardson et al. (2000), meddies have radii from 10 to 50 km and are typically 500–1000 m thick. Bower et al. (1997) estimate that 17 meddies form per year from the Mediterranean outflow waters. All known meddies have been anticyclonic, although some observations suggest nearby companion cyclonic partners. Typical meddy salt and temperature anomalies are 0.4–1.1 psu and 2.0–4.0°C, and typical meddy depths are near 1100 m. Meddies are further highly inertial as suggested by their observed Rossby numbers of -0.2 (Schultz-Tokos and Rossby 1991, STR hereinafter).

Because of several documented life histories (e.g., Armi et al. 1989; Richardson et al. 1989; Richardson and Tychensky 1998, RT hereinafter); it is now widely accepted that the open-ocean decay of meddies is slow and consistent with multiyear meddy lifespans. In contrast, topographic interactions appear to provide meddies with a fast path to decay (RT). Two topographic features block open-ocean meddy migration: the Horseshoe Seamounts and the Great Meteor Seamounts (see Fig. 1). The Horseshoe Seamounts are a curved grouping of near-surface-reaching seamounts located southwest of Cape St. Vincent. This seamount chain is the primary topographic obstacle facing many newly formed meddies. The Great Meteor Seamounts constitute a significant topographic anomaly of the Mid-Atlantic Ridge with which several meddies have also been observed to interact (Richardson et al. 2000).

Meddy–seamount interaction has been well documented in float data, from which it appears they catalyze significant exchange between meddies and the background North Atlantic. The interactions can be quite disruptive to meddy structure, leading possibly to destruction. Although this is apparently not the only outcome (Shapiro et al. 1995, S95 hereinafter; RT), meddy–seamount interactions have been suggested as potentially significant, and perhaps dominant, in the maintenance of the Mediterranean salt tongue (RT). Support for this also comes from some straightforward estimates. The mean salt equation is

$$\overline{\mathbf{u}} \cdot \nabla \overline{S} = -\nabla \cdot (\overline{\mathbf{u}' S'}), \tag{1}$$

where overbars denote mean state quantities and primes are deviations from means. The left-hand side was estimated on (almost) neutral surfaces by Armi and Stommel (1983) for the Mediterranean tongue, using β experiment data, to be

$$\overline{\mathbf{u}} \cdot \nabla \overline{S} \sim (-2.0 \pm 1.0) \times 10^{-10} \text{ psu s}^{-1}. \tag{2}$$

This value was for a flank region of the tongue but is assumed here as characteristic of the entire feature.

All eddy processes are included on the right-hand side, one of which is meddy–seamount interaction. Using modest meddy values, the total meddy-induced salt anomaly transport for the eastern Atlantic is

$$17 \text{ meddies yr}^{-1} \times \pi(30 \text{ km})^2 500 \text{ m} \times 0.4 \text{ psu} = 3.1 \times 10^5 \text{ psu m}^3 \text{ s}^{-1}. \quad (3)$$

Of the 17 meddies formed per year, about 15 experience seamount encounters (Richardson et al. 2000). Assuming these are destroyed, the net salinity deposition into the eastern Atlantic is 86% of the above number. The area of the Mediterranean salt anomaly is roughly 17° by 17°. Thus the above transport, if mixed over this area and adjusted for the anomalous thickness between the density surfaces found in meddies, represents a net ''turbulent'' flux divergence of

$$3.0 \times 10^{-10} \text{ psu s}^{-1}, \quad (4)$$

which is bigger than but comparable to the advective flux divergence.

This order of magnitude estimate argues, first, that salt transport by meddies is strong enough to maintain the Mediterranean salt tongue and, second, that meddy–seamount interaction is an important Mediterranean salt tongue maintenance mechanism. This latter point sets the central question of this paper. Specifically, meddy–seamount encounters can range from fatal to glancing or off-center collisions resulting in a ''wounded,'' but largely intact, meddy. Survival of this kind reduces the effective meddy release and lessens their impact on the salt tongue. The goal of this study is to assess the efficiency of meddy–seamount interaction in enabling meddy salt flux to the salt tongue.

While the general area of topography–eddy modeling has received prior theoretical and modeling attention, the specific area of vortex seamount interaction has not been much explored. Simmons and Nof (2000) computed the minimal conditions necessary to split vortices by topographic barrier encounters. The inclusion of baroclinicity, multiple seamounts and filamentation in the present study extends their work. Herbette et al. (2003), in work conducted in parallel with the present effort, have computed surface vortex interaction with sizable bottom bumps in a primitive equation model. Here, we are concerned with seamounts interacting directly with the primary vortex core.

Accordingly, we argue that meddies have a surprising ability to survive seamount encounters, even in the strong interaction limit in which the meddy core is split by the seamounts. The meddy remnants, depending upon the details of the interactions, can reorganize by the mechanics of like-signed vortex merger and vortex regularization into one or two cores in which significant fractions of the initial meddy volume can be captured. Some comparable results appear in Herbette et al. (2003). We estimate that, on average, 35% of the meddy core is irreversibly lost by seamount encounters. This is associated with a significant input into the Mediterranean salt tongue, but other mechanisms appear to be necessary to close the salt tongue budget. Locally, seamount impact can account for most of the required salt flux near the Horseshoe Seamounts but has little affect near the Great Meteor Seamounts.

Thus our results imply vortex survival is a limiting influence on the Mediterranean salt tongue. In other words, the vortices emerging from seamount impact export the bulk of the meddy salinity anomaly to the rest of the North Atlantic, rather than depositing it locally. Because of the effect of this divergence on the amplitude of the salinity anomaly, this behavior has implications for global climate modeling.

The paper is organized as follows. A quasigeostrophic point vortex numerical model is developed in the next section and the experimental set up is described. The results from our experiments are described and analyzed in section 3, and the paper ends with summary and discussion sections.

2. Model development

Some of the controlling parameters of our problem are suggested by Fig. 2, which is a view of the North Atlantic topography looking westward from the coast of Africa at roughly 28°N. Also shown in this figure are the approximate size and depths of three observed meddies, both of which serve to argue the almost inevitability of North Atlantic meddy–seamount interactions.

For later use, note that the seamounts are extremely steep features with widths and gaps comparable to the lateral scales of the meddies.

Standard gridpoint methods could be used to model the problem of meddy–topography interaction; however, we have opted here to use a point vortex approach. This method, by way of review, exploits potential vorticity conservation to examine inviscid solutions of the quasigeostrophic equations. The inviscid, three-layer, unforced, quasigeostrophic (QG) equations on an f plane are

$$\frac{d}{dt}q_i = 0, \qquad i = 1, 2, 3,$$

$$q_i = \frac{\nabla^2 p_1}{f_o} + \beta y - f_o \frac{p_1 - p_2}{g' H_1},$$

$$q_2 = \frac{\nabla^2 p_2}{f_o} + \beta y + f_o \frac{p_1 - p_2}{g' H_2} - f_o \frac{p_2 - p_3}{g'' H_2}, \quad \text{and}$$

$$q_3 = \frac{\nabla^2 p_3}{f_o} + \beta y + f_o \frac{p_2 - p_3}{g'' H_3}, \quad (5)$$

where f_o denotes the Coriolis parameter, H_i is the av-

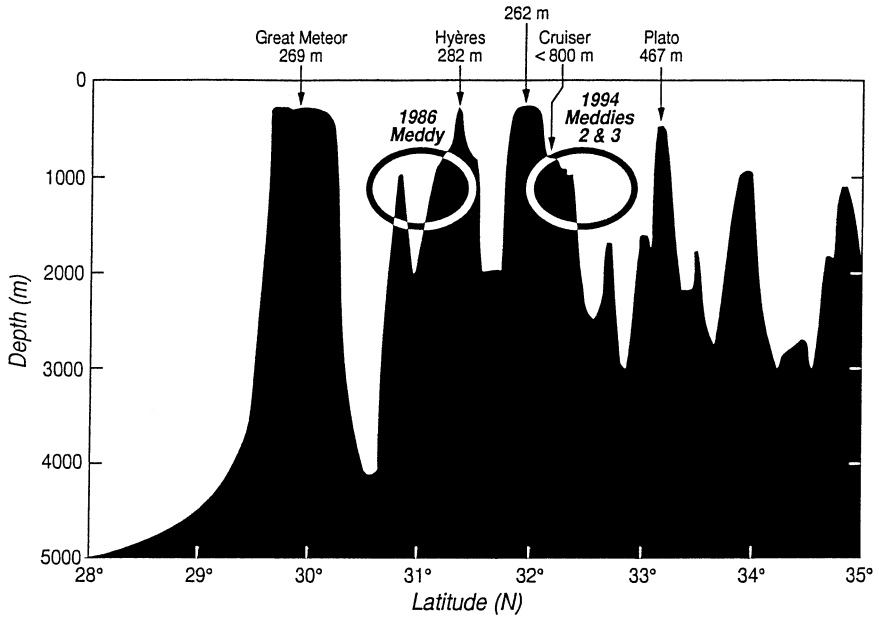

FIG. 2. Meddy–topography interaction. This is a westward-looking view showing the Great Meteor Seamounts along with the approximate location in the water column of three observed meddies (courtesy of P. Richardson.)

erage thickness of layer i, p_i is the ith layer pressure, d/dt is the quasigeostrophic material time derivative,

$$\frac{d}{dt} = \frac{\partial}{\partial t} + \frac{1}{f_o} J(p_i, \cdot),$$

and g' and g'' are the reduced gravities of the two interfaces. Velocities are related to pressure by geostrophy.

An exact solution to (5) is

$$q_i(\mathbf{x}, t) = q_i(\mathbf{x}_0, 0) \quad \text{and} \quad \mathbf{x} = \mathbf{x}_0 + \int_0^t \mathbf{u}(\mathbf{x}, t)\, dt, \qquad (6)$$

which expresses the conservation of potential vorticity by fluid parcels. Given a distribution of q_i, pressure can be obtained by inverting (5), and the system can be advanced in time using (6). The potential vorticity field is discretized into parcels whose interactions are computed using a Green's function approach. The potential vorticity patch evolves in time as the advection field established by the point vortex collection stirs the point vortices. Further details on the calculation are given in Dewar (2002), and extensive testing is discussed in Wang (2001).

The point vortex method has been used traditionally to study vortex evolution in flat-bottomed, f-plane settings. Here we modify the setting by including idealized seamounts in the form of right circular cylinders that span the entire water column; a schematic of model geometry appears in Fig. 3. The neglect of β, implicit in the point vortex approach, can be rationalized by scaling; also Nof's (1981) estimate of the β-induced meddy drift is weak. Strengths of the point vortex approach for meddies are that it emphasizes inertia, whose importance is suggested by observed meddy Rossby numbers, and that it permits the seamount boundary to be captured analytically. Because of the latter point, we are free of numerical issues surrounding boundary representation. We model meddies as clouds of point vortices, rather than using contour dynamics, in order to avoid the contour distortion and breaking caused by seamount encounters.

There are at least two weaknesses of the point vortex method deserving explicit mention. First, internal waves are probably generated during meddy–seamount interactions, and these are not included here. On the other hand, internal waves appear in other QG and primitive equation models as friction, and it is not clear that this is valid. Also, the interaction timescales of meddies and seamounts are relatively short (from weeks to a few months), and so it is unlikely potential vorticity is strongly modified by the encounter. Second, and probably more important, finite slopes on the seamounts are neglected. This is justifiable if the lateral scale over which the seamount rises to the surface is small in comparison with a deformation radius, but not all of the Mediterranean regional seamounts are well described in this way.

Experimental design

Float data have shown interactions of meddies with either one or two seamounts, and so we confine our studies to these cases. A barotropic westward mean flow

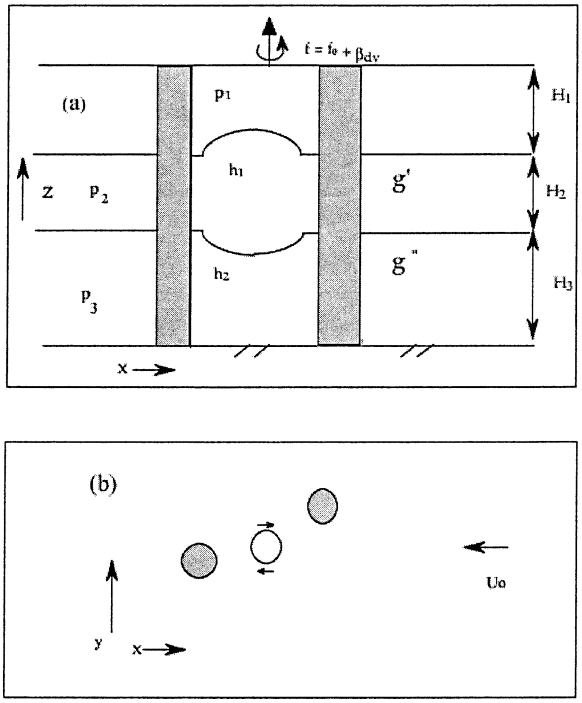

FIG. 3. Model schematic that shows a three-layer configuration: (a) side and (b) plan views. The model topography consists of several seamounts, here modeled as right circular cylinders. Notation is standard.

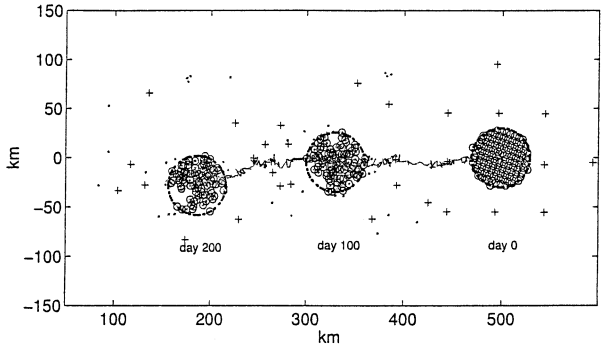

FIG. 4. Meddy snapshots at days 0, 100, and 200 during initialization. A background advection of -0.02 m s^{-1} accounts for the westward vortex displacement. The open circles are the anticyclonic vortices and the $+$, $\times$, and $\cdot$ mark the cyclonic vortices at the successive dates. The circle centered on each vortex has a radius of 30 km. The jagged line traces the vortex center of mass.

is used to advect the meddies into the seamount near field: we used a value of 0.02 m s^{-1}, which is similar to the observed speeds of meddy migration. Stern (1999) employed a similar strategy in a study of barotropic vortices. We study three-layer models with the meddy embedded in the middle layer. Layer thicknesses were taken as 1000, 500, and 1000 m for the top, middle, and bottom layers respectively, and the reduced-gravity parameters were both 0.01 m s^{-2}. These result in deformation radii of 32 and 14 km. Both are similar to those of the area in which meddies are observed. The meddy potential vorticity anomaly used here is set to $0.2 f_o$: meddies so generated have anticyclonic swirl speeds of 0.2 m s^{-1} and maximum Rossby numbers comparable to, but slightly less than, the observed -0.2 (STR). The meddy initial radius was set to be 30 km (meaning anticyclonic point vortices were initially uniformly distributed inside a circle of 30-km radius), consistent with meddy observations and also comparable to the first deformation radius.

Meddies are observed to enter into near-field interactions with seamounts. ''Unshielded'' vortices, that is, vortices with nonvanishing integrated barotropic potential vorticity anomaly, tend to avoid seamounts by means of far-reaching barotropic interactions. To prevent this unrealistic behavior, we ''shielded'' our meddies using cyclonic point vortices in the same layer as the meddy anticyclonic anomaly. Weak cyclonic point vortices positioned outside the meddy core, when distributed over large areas, can efficiently cancel net barotropic potential vorticity. The flows associated with the cyclonic part of the meddy are thus weak, in keeping with observations.

All our initial radially symmetric vortex configurations were unstable (Flierl 1988), and so we permitted the vortex to evolve into a robust state prior to initializing seamount encounters. This state, while not perfectly symmetric, was long-lived and involved almost all initial point vortices. An initialization sequence appears in Fig. 4, where locations of all the point vortices for days 0, 100, and 200 are shown. In all cases, a circle of radius 30 km is included about the estimated center of mass of the core point vortex to illustrate the point vortex grouping identified with the coherent eddy. The eddy center of mass trajectory appears as the jagged line and is dominated by the -0.02 m s^{-1} westward advection. A slight southward shift associated with the unstable eddy evolution is also seen.

Vortex snapshots from late in the initialization run were used to initialize our meddy–seamount interaction experiments. The dominant anticyclonic vortex was located and its center of mass was computed. This location was used as the vortex center when positioning it in the various experiment sets.

Considerable vortex distortion often occurred during vortex–seamount interaction. In general, however, the bulk of the point vortices moved beyond the influence of the seamounts and eventually settled into a robust structure, consisting of one or more coherent vortices and residue. The large number of interacting point vortices involved makes the system, not surprisingly, sensitive to initial conditions. Slight differences in the impinging vortices could result in observable differences in the long-term evolution. We therefore conducted ensembles of experiments within each seamount configuration to obtain statistically reliable results. The ensembles were constructed by reinitializing the experi-

ment sets using the initialization run at days 190, 192.5, 195, 197.5, and 200.

Vortex size was gauged by counting the number of point vortices found in coherent structures. It was necessary to automate this given the large number of experiments, and so an algorithm was developed to identify coherent point vortex populations. In brief, the algorithm counts the point vortices in circular regions of one deformation radius and identifies the largest concentrations. The technique is described in more detail in the appendix. In many cases, the results were found to be consistent with manual counts.

The seamount radii used here are 30 km. This is comparable to the vortex size, in keeping with the observations. We have investigated single and double seamount configurations. Note in Fig. 2, typical seamount gaps are around 70 km. We have studied double seamount settings with gaps of 30, 40, and 50 km, which if anything tend to overemphasize the role of multiple seamount interactions.

In all cases, the meddies are placed 200 km east of the seamount complex, a distance at which they appear to be unaware of the seamounts. The experiments are typically integrated for 200 days, giving more than 100 days of meddy–seamount interaction. A small number of integrations were continued beyond 200 days to clarify the long-term fate of the vortices.

3. Experimental results

We first describe meddy–single seamount interaction. Although meddies appear to have preferred zones of propagation (Richardson et al. 2000), their approach to seamounts differs from encounter to encounter. We thus modify the initial meridional upstream vortex location relative to the seamounts. A total of 101 experiment sets were conducted in each of our seamount configurations. For the single seamount setting, the initial vortex was varied north–south relative to the seamount center at increments of 1 km. It was found that for initial vortex placements at the northern and southern extremes of the range, seamount effects on the vortex were weak. This suggests our experiments span the range over which seamounts constitute a significant input to vortex evolution. Although our numerical technique permits general seamount spatial distributions (e.g., as shown in Fig. 3), we have studied only seamounts aligned perpendicularly to the mean flow. For dual-seamount settings, the seamounts were situated symmetrically about 0 km and the vortex centers were displaced meridionally relative to that point.

a. Experiment set I: Single-seamount encounters

This set of experiments displayed two modes of long-term meddy behavior. The dominant mode was that the vortex core survived as a single eddy in spite of, at times, considerable distortion in the vortex structure.

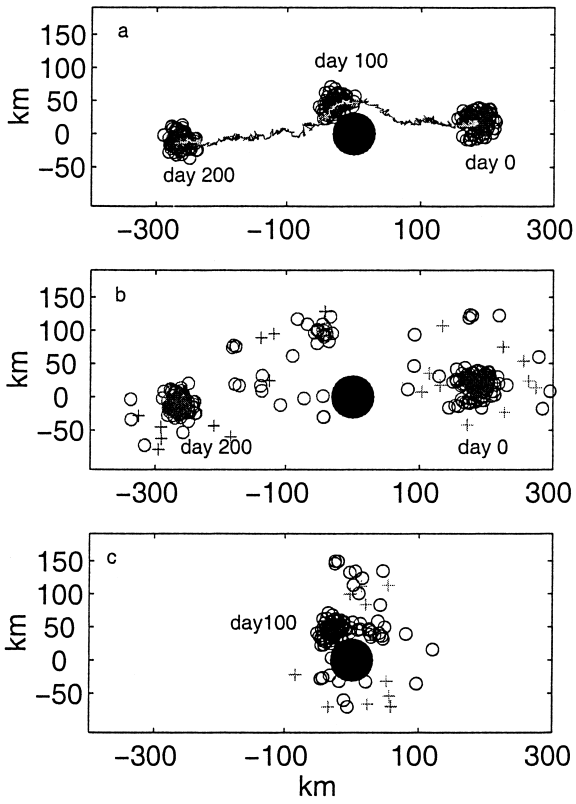

FIG. 5. The initial vortex location is (200 km, 19 km) relative to the seamount center. (a) The meddy center-of-mass trajectory (jagged line) with superimposed point vortex core distributions at days 0, 100, and 200. Only the point vortices identified as coherent appear. The locations of all 123 vortices for (b) days 0 and 200 and (c) day 100 (+ marks the cyclonic vortices). They show the degeneration of the primary meddy into a primary coherent vortex, a secondary weak vortex, and residue. The secondary vortex here is excluded from our survival count because it does not exceed our threshold criteria.

Two extreme examples of such evolution appear in Figs. 5 and 6. In these experiments, the meddies were located initially 19 km north and 42 km south of the seamount center.

The point vortices in the coherent vortex at days 0, 100, and 200 appear in the upper panel of Fig. 5. The eddy center of mass trajectory (jagged line) shows cyclonic movement east of the seamount. This is caused by the reaction of the vortex and mean flow fields to the seamount. The mean flow splits symmetrically around the seamount, while each point vortex in the approaching meddy sees a cyclonic image produced by the seamount boundary. The character of the movement is consistent with a finite near-field interaction, as is observed, and also argues for this setting that meddies attempt to dynamically avoid seamount interaction.

The locations of all the point vortices (i.e., not just those associated with a coherent structure) at days 0 and 200 appear in the middle panel, and those from day 100 are in the bottom panel. Comparing panels shows the difference between coherent vortices and residue. This

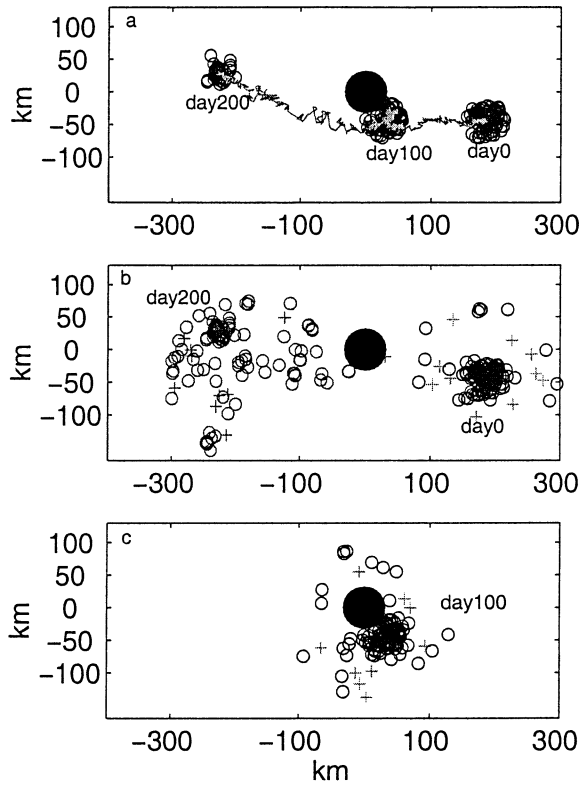

FIG. 6. Meddy–seamount interaction. As in Fig. 5 but the initial vortex was located at (200 km, −42 km) relative to the seamount center. The meddy is significantly damaged by this encounter, losing about 50% of its constituent vortices.

is an example of a rather mild interaction with a seamount; most of the point vortices inside the initial vortex are retained. There is a weak splinter vortex at day 200 located just northwest of the seamount (see middle panel), but this is a minor feature.

Figure 6 is an example of a far stronger interaction with the topography, where the structure of the vortex is distorted considerably near the seamount. In this case, the loss of coherent vortex mass is far greater than that seen in Fig. 5, yet the long-term state still contains an identifiable coherent structure (upper panel). This experiment exhibited the greatest loss of mass from the coherent structure of any of our single-seamount experiments. Approximately one-half of the initial core meddy vortices are lost from the emergent eddy. Note, however, that the day-200 coherent vortex is compact, indicating the core potential vorticity anomaly of the eddy is comparable in magnitude to its initial value. The final radius of the coherent vortex is roughly 15 km, which, while small, is within the range of observed SCVs.

The details of the weaker meddy interaction with the seamount appears in Fig. 7, where snapshots of point vortex locations at 10-day intervals between days 65 and 115 are shown. The dominant tendency is for the vortex to circle the seamount cyclonically and for the bulk of this trajectory to occur with minimal actual contact of the meddy with the seamount. This behavior is characteristic of nearly all of the experiments and is due to the effect of the image vortices inside the seamount on the impinging meddy. There is some distortion of the eddy core during its transit of the seamount, but it is successfully resisted by the tendency for the core to hold together. A return to near-circular symmetry occurs shortly after the vortex leaves the vicinity of the seamount because of vortex regularization.

The strong meddy–seamount interaction case appears in Fig. 8. The impinging vortex begins a slight cyclonic movement, due to near-field interaction, as it nears the seamount. Rather than repulsive, this interaction is attractive, drawing the vortex into the seamount boundary. The vortex subsequently stagnates in the near neighborhood of the cylinder boundary. It is held together by the integrity of its core but undergoes constant distortion due to the shearing effects of the mean flow and the vortex images. The outer point vortices are stripped away during this period, reducing the size of the coherent anticyclonic core. Eventually the core becomes too weak to maintain its position against mean advection, and a reduced core is swept anticyclonically about the seamount. This core continues as a coherent vortex whose core population grows slightly between days 165 and 200 because of like-signed vortex merger (Christiansen and Zabusky 1973). Our tracking scheme estimates it has a little more than one-half of its precollision point vortex population at the end of the experiment.

The second mode of long-term behavior consisted of the initial vortex splitting into two sizable coherent vortices and residue. An example of this behavior appears in Fig. 9, from an experiment with an initial vortex at (200 km, −26 km).

Details of the latter interaction appear in Fig. 10, where plan views of all the vortices are shown. The separation between subsequent plots is 20 days, and the sequence begins at day 65. Again there is considerable distortion of the core around the seamount as the vortex effectively breaks. The organizing tendencies of the like-signed anticyclonic vorticity however holds together clumps of the initial vortex, permitting two groupings of like-signed vorticity to exit the seamount. These clumps, each contained within a deformation radius, form the nuclei from which the subsequent vortices emerge. There is also evidence of core population growth between days 165 and 200 for both coherent eddies.

Given that real ocean meddies are strong potential vorticity anomalies and their period of interaction with topography is relatively short (e.g., RT), it is tempting to think only small frictional modifications of their anomalies can occur. This idea is reinforced even more if the distortion occurs without much actual contact of the Meddies with the seamount topography. Under this scenario, the postinteraction field in the real ocean

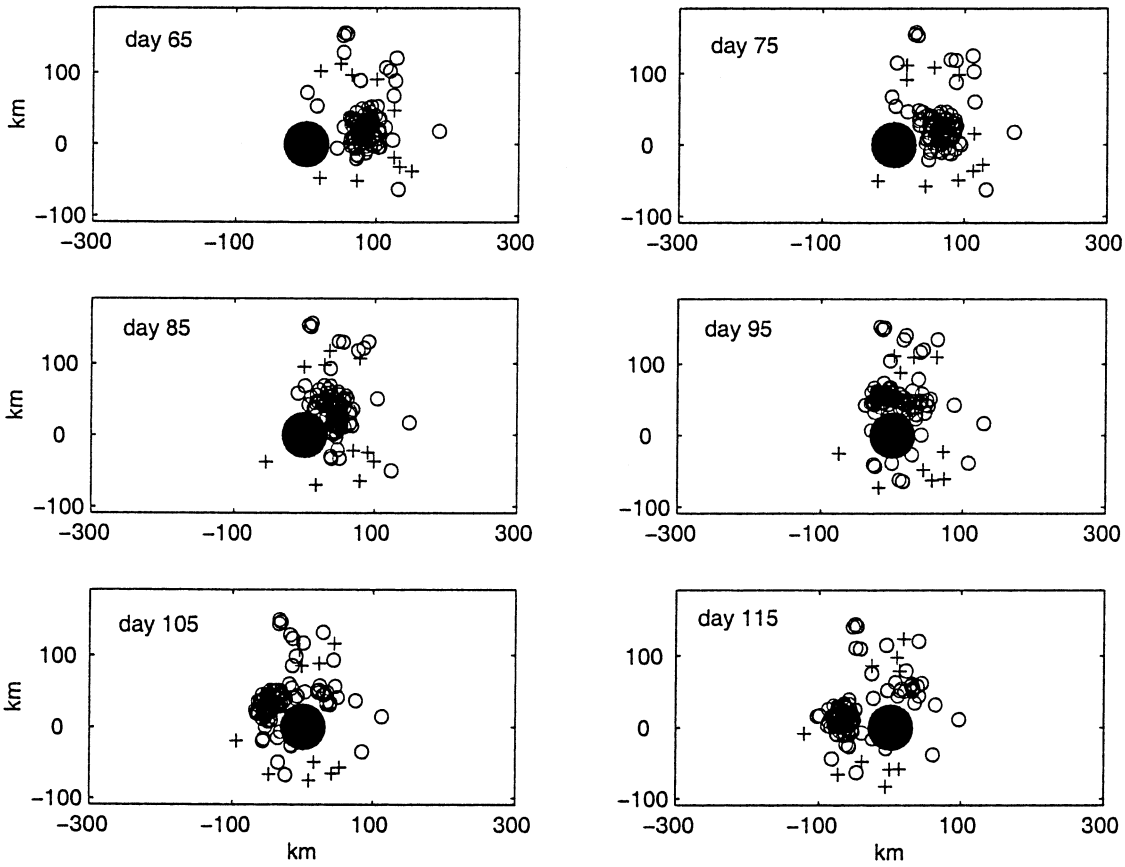

FIG. 7. Vortex cloud plots at 10-day intervals during meddy–seamount interaction. This vortex was begun at (200 km, 19 km). The distortion of the core is minimal, with the bulk of it taking a cyclonic path about the seamount. This path is induced by the cyclonic images of the vortex in the seamount. A core eventually separates from the seamount, the population of which is comparable to the vortex initial population. The o represent the anticyclonic point vortices and the + are the cyclonic point vortices.

should still consist of large-amplitude potential vorticity anomalies capable of reorganization.

b. Survival ratio estimation

The final coherent structure point vortices count is divided by the initial meddy point vortex population to yield a ''survival'' ratio. Roughly speaking, this number measures the volume of the initial meddy that ultimately survives the seamount impact as a coherent structure. It was found the ratio did depend on the initial conditions used for the meddy, thus ensembles of experiments were conducted. The survival ratios for ensemble sets as a function of initial vortex location were averaged to give mean survival ratios.

Survival ratio data for the single-seamount experiments appears in Fig. 11. The top panel shows averages computed from the ensembles (dot–dash line) and the lower panel shows survival ratio variance within the ensemble. Note the ensemble mean in the upper panel is somewhat noisy, so we also performed a five-point running average of the ensemble mean results. This line appears in Fig. 11 as the solid line. The upper-panel outer curve plots total survival ratio as a function of initial meddy location relative to seamount center; the inner curve indicates the survival fraction found in smaller second vortices. This plot is consistent with the two primary modes of meddy behavior discussed above in that, when the meddy is relatively far north or south of the seamount center, it survives the interaction with most of its core intact. The survival ratios in these regimes are approximately 0.8–0.9 and correspond to Figs. 5 and 7. The second regime consists of the appearance of two coherent vortices in the wake of the interaction. This occurs for the area where the meddy center is relatively close to, but slightly south of, the topographic center and is indicated by the appearance of the inner curve.

The variance about the ensemble mean values is indicated in the upper panel and also appears separately in the lower panel. In the latter, the solid curve is the variance of the total count and the dashed curved is the variance of the second vortex survival rate. The interesting structure here is the large variance found for ini-

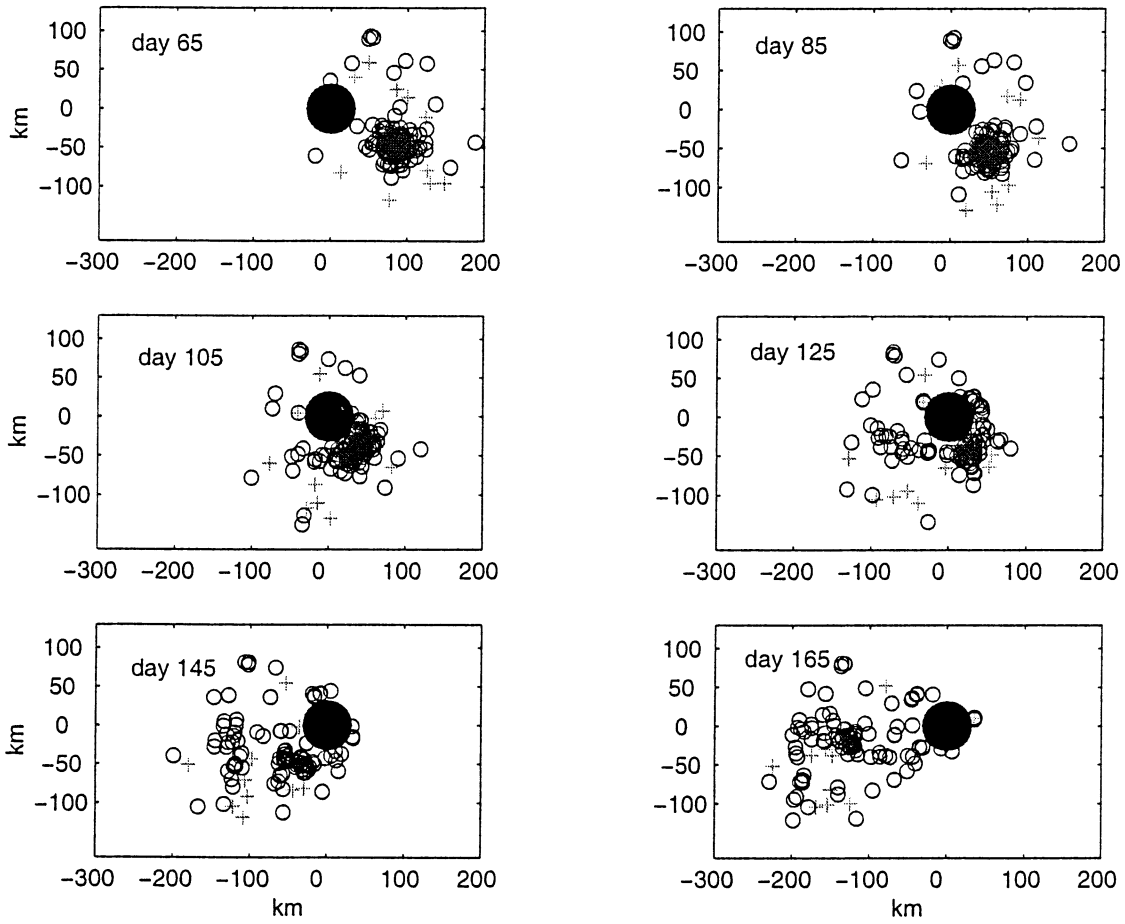

FIG. 8. Vortex cloud plots at 20-day intervals during meddy–seamount interaction. This vortex started at (200 km, −42 km). The distortion of this core is considerably greater than in the previous case, with the vortex effectively stagnating against the seamount for about 60 days. The stagnation represents a balance between the anticyclonic advection due to the mean flow and the cyclonic-image-induced tendencies of the vortex.

tial vortex locations from −20 to −50 km, that is, near the southern edge of the seamount. This location corresponds to Figs. 6 and 8 where considerable distortion and shredding of the vortex was seen. For impinging vortices contained within the window of high variance, the outcome of the collision is difficult to predict. Either one or two vortices can emerge, and their respective sizes can vary. Total survival rates are also variable, although the range is confined between 0.5 and 0.7. For vortices outside this window, the outcomes look reasonably predictable. The bulk of the vortex typically survives as a single coherent structure with about 80% of the initial mass intact.

Averaging the survival ratio across the initial conditions shows that typically 70% of a meddy survives an interaction with a single seamount as some type of coherent vortex.

c. *Experiment set II: Two seamounts*

For the 30-km seamount spacing, the meddies were placed from −67 to 33 km; for 40 km, the settings were −72 to 28 km; and for 50 km, they were −77 to 23 km. Experiments with settings outside these ranges yielded results like the single seamount experiments.

Although two cylinders made the evolution more complex, some common characteristics between these and the single-seamount experiments were found. The biggest distinction was that the fission of the meddy into two coherent structures was far more likely, with a probability inversely proportional to seamount separation. An example of such an interaction appears in Fig. 12. In this case, the meddy started at (200 km, −6 km) and interacted mostly with the northern seamount. It is interesting to contrast this experiment with the comparable single-seamount experiment, where the initial meddy location relative to the single seamount was the same as the initial location in the present experiment relative to the northern seamount. In the single-seamount cases, the meddy did not split into two coherent vortices, illustrating the role of the southern seamount.

Details of the seamount–vortex interaction in this case appear in Fig. 13 showing point vortex snapshots at 10-

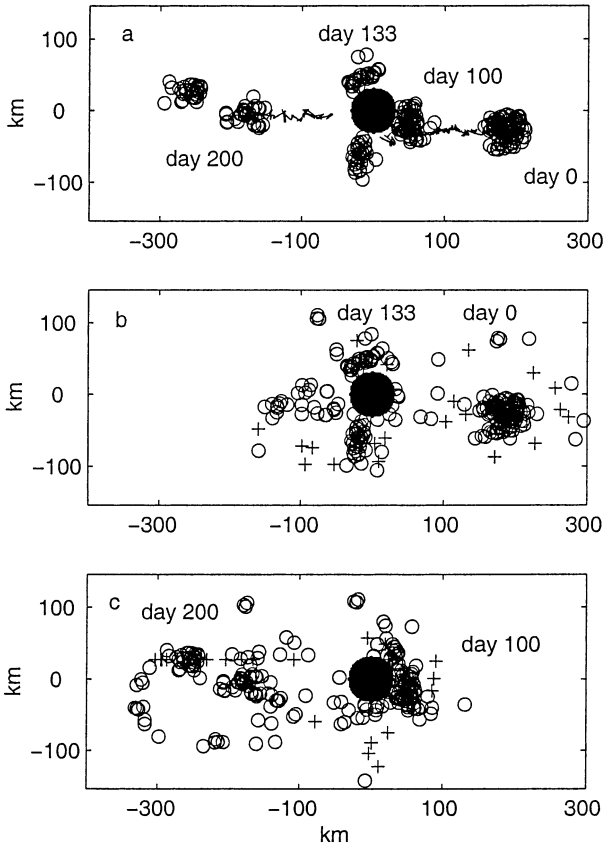

FIG. 9. As in Fig. 5 except the vortex was initially at (200 km, −26 km). (a) The center-of-mass trajectory (jagged line) with views of the core point vortices from days 0, 100, 133, and 200. All point vortices from (b) day 0 and 133 and (c) days 100 and 200. Note the emergence of two coherent vortices after the collision.

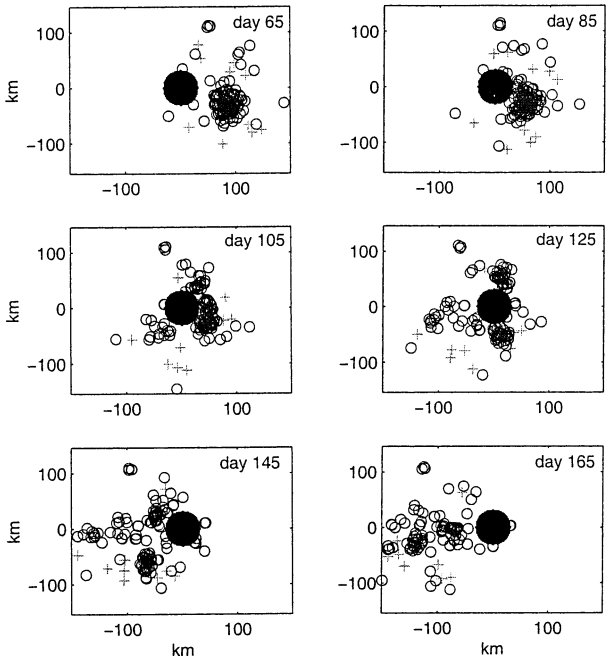

FIG. 10. Vortex cloud plots at 20-day intervals, beginning at day 65, during meddy–seamount interaction. This vortex started at (200 km, −26 km). This case displays the second dominate mode of vortex behavior, i.e., meddy fission into two vortices. Core loss occurs, as evidenced by the leading stream of potential vorticity seen on day 125.

day intervals. The dynamic presence of the second seamount is clear. Note also the like-signed vortex merger occurring between days 110 and 130. Specifically, the coherent vortex emerging from the interseamount passage is led by several point vortices that, in the later panels, are absorbed into the coherent structure.

Figure 14 shows survival ratios for seamounts 30 km apart. In this case, the meddies split essentially all initial conditions. These results are ensemble averages of the five experiment sets discussed above. Also shown are five-point smoothings of both lines, which were used to compute variances as a function of initial vortex location. These curves show that the lowest survival rates occur for meddies incident on the southern flank of the southern seamount. Such meddies experience strong interactions with both seamounts due to an initial cyclonic drift toward the interseamount passage.

In Fig. 15, survival ratios for a separation of 40 km appear. In this case, survival as a solitary vortex was more likely, while in Fig. 16 (for seamount separations of 50 km), the meddy could often experience the seamount complex essentially as a single seamount interaction. Based on these experiments, we suggest that the

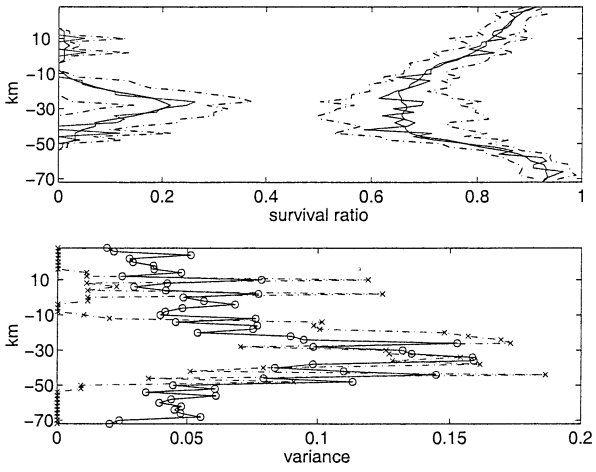

FIG. 11. Meddy survival rate after collision. (top) The *y* axis is the initial vortex location relative to seamount center and the *x* axis is the point vortex fraction surviving the encounter. The line on the right represents the total coherent vortex survival count; the left curve represents the fraction found in a second core. The solid lines are averages over ensembles, variance about those averages are indicated. (bottom) Variance of the survival ratio as a function of initial meddy location. The solid line is variance of the total survival ratio, and the dashed line is variance of the fraction in the second vortex.

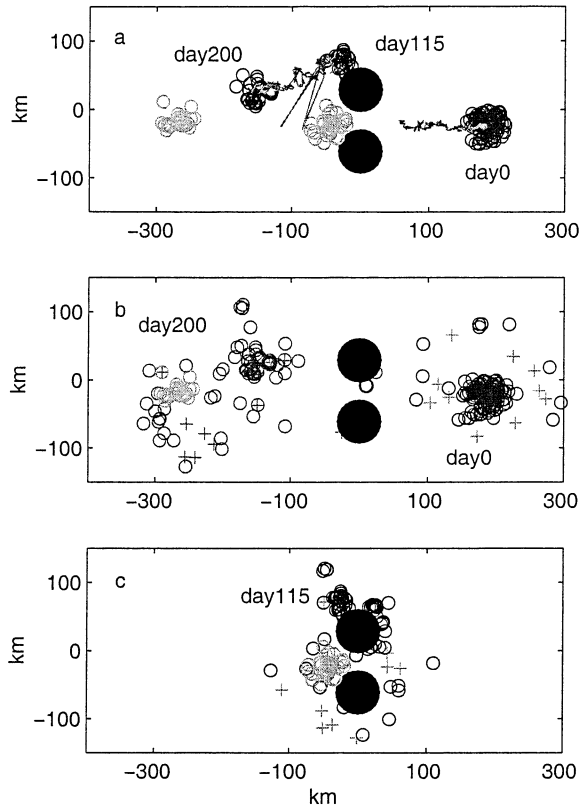

FIG. 12. Meddy interaction with two seamounts (30-km gap). (a) The core point vortices at days 0, 115, and 200 superimposed on the center-of-mass trajectory of the vortex. All the point vortices from (b) days 0 and 200 and (c) day 115. The initial meddy splits into two meddies in this experiment, following the typical evolution sequence for the two-seamount case.

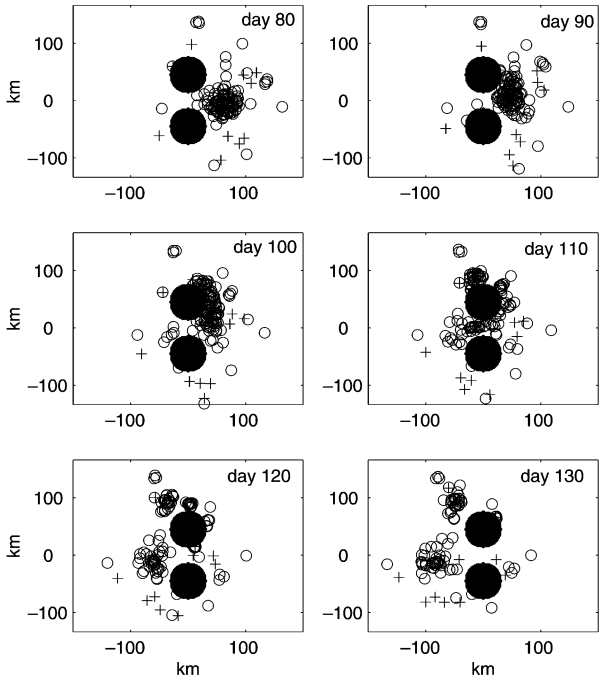

FIG. 13. As in Fig. 6 but for a two seamount case and a meddy initially at (200 km, −6 km). Plan views of vortex locations appear at 10-day intervals beginning on day 80. The initial meddy splits into two meddies in this experiment and thus follows the typical evolution sequence for the two-seamount case.

critical gap between seamounts necessary to dynamically separate their effects is roughly 45–50 km, that is, about 1.5 deformation radii. Given that most major seamounts are at least 50 km apart, the single-seamount-interaction scenario seems very relevant to meddy survival.

The formation of three vortices was observed in a small number of cases when the southern seamount by itself split the incident meddy. One core then propagated anticyclonically about the seamount, while the second core moved northward into a region where it was influenced by the northern seamount. This interaction could further split the second core, although the cores were unequal in size. None of the third cores were included in our survival statistics because they did not exceed the threshold criteria of our counting procedure (see the appendix).

The survival rates, averaged over all initial conditions, from each experiment set appear in Table 1. The highest average survival rate, 0.78, comes from the single-seamount cases; the rates for the two-seamount experiments increase from 0.62 for the smallest separation to 0.68 for the largest. In all cases, the reorganization of the interacted meddy into postcollision coherent vortices is quite strong. Averaging the survival rates over all experiments yields 0.67 as a measure of meddy survival of seamount interactions under broad conditions. The combined effects of advection and images in these

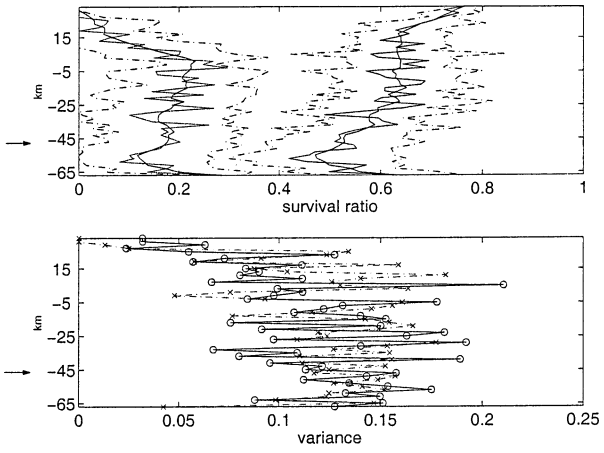

FIG. 14. As in Fig. 11 except two seamount experiments are shown. The seamount separation is 30 km, and the arrow denotes the center of the southern seamount (the northern seamount was centered at 45 km north). The outer line represents the net survival ratio after the collision, including the two biggest cores (subject to our acceptance criteria). The inner line is the fraction contained in the smaller core. The light solid curves are ensemble averages over five sets of experiments. Also shown are five-point smoothings of the light curves (heavy solid lines). Variances were computed relative to the heavy lines.

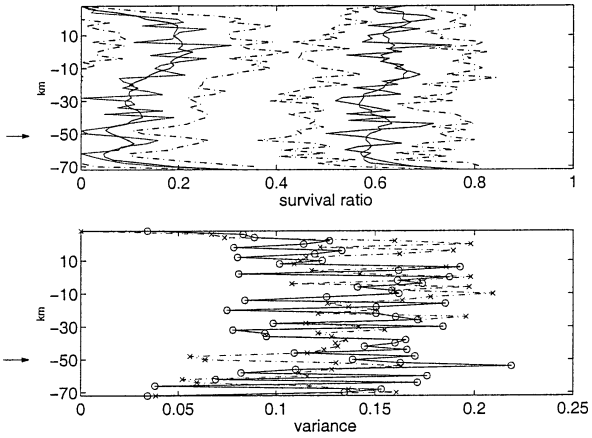

FIG. 15. As in Fig. 14 except the seamount separation is 40 km.

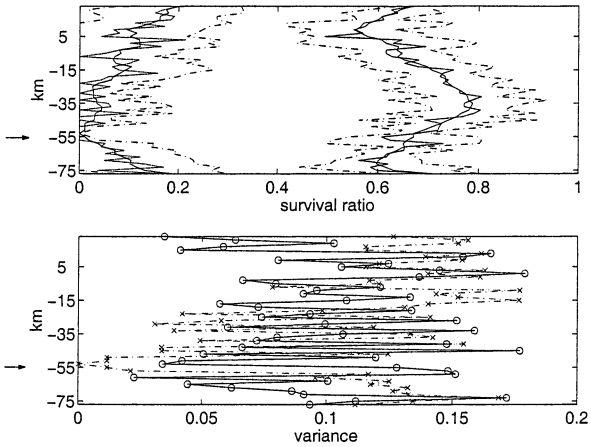

FIG. 16. As in Fig. 14 except the seamount separation is 50 km. Note the likelihood of a single surviving vortex is similar to the single-seamount experiments.

experiments renders the window where the vortices can be severely shredded to confined zones southeast of the seamount. Second, the robust tendency of like-signed vortex anomalies to reorganize into vortices and merge causes the emergent vortex anomalies as they exit the seamount locations to regularize into a coherent structure. An aid in this process is the extreme and strong potential vorticity anomaly represented by meddies.

This number is possibly an underestimate of survival. It includes results from several experiments in which seamounts are more closely spaced than observed. This biases the outcome toward low survival. Several small vortex structures are also excluded from our survival counts primarily because of size. While this may be reasonable, some long-lived structures may be excluded. In any case, an overarching statement is that roughly 65% of the volume initially in a meddy impinging on a seamount can be expected to survive in coherent vortices.

4. Discussion

This study has examined meddy–seamount interaction in order to quantify the impact of such events as meddy life history. The experimental design was modeled after the observed system, while remaining a process study. Of the various components of the study, the two that, in our opinion, are most in need of further work are the sensitivity of the result to the barotropic advection field and the absence of finite seamount slopes. We hope to persue these in following studies, but we press on here with comparisons between our results and data.

a. Comparisons with direct observations

Shapiro et al. (1995), RT, and Richardson et al. (2000) describe open-ocean meddy–seamount interactions that can be compared with our results. S95 reported on Meddy Irving that interacted with two seamounts rising to depths of 300 m and separated by roughly 90 km at typical meddy depths. Our calculations argue that a likely outcome of the interaction would be the survival of the bulk of the meddy in a postcollision vortex. S95 report that after passage between the seamounts, an elliptical vortex followed by a wake of saline water was observed. The authors interpreted the vortex as a survived meddy and also noted two small salty patches within the meddy wake whose temperature and salinity characteristics matched those of the primary core. From data the authors concluded somewhere between 20% and 30% of the initial vortex mass was lost as a result of the seamount interaction. This agrees well with our expected survival ratio of 0.65. We might even speculate that the observed oblong vortex (major-to-minor axis ratio of about 2) was a meddy knocked away from a more symmetric configuration by seamount distortions and in the process of regularizing again by vortex mechanisms.

Richardson and Tychensky (1998) and Richardson et al. (2000) discuss several meddies ''seriously wounded'' by seamount interactions. A very interesting time series is the temperature data from Meddy 26, which after collision with Cruiser Seamount, dropped from roughly 12.8° to 8.1°C. These data are suggestive of strong entrainment and mixing of meddy core water with the background. Our calculations are consistent with this in the sense that strong interactions, which the float tra-

TABLE 1. Meddy survival rates. Averages over all initial conditions for single-seamount and two-seamount experiments (as a function of interseamount separation) are shown. Two-seamount experiments have lower servival rates than the single-seamount experiment. The average of all cases is roughly 0.65.

Expt	Seamounts	Separation (km)	Survival rate
a	1		0.78
b	2	30	0.62
c	2	40	0.62
d	2	50	0.68

jectory supports, always result in meddy core loss. We would therefore interpret this float as having been part of the (up to) 50% of the meddy core that was irreversibly separated from the meddy by the seamount. Richardson and Tychensky (1998) also discuss meddy bifurcation due to seamount interaction. Although many details of the meddy and the interaction do not fit our model design, fission is a frequently observed model end state.

Another meddy, (Meddy 1) apparently survived an encounter with Plato Seamount, a 15-km radius seamount extending to within 470 m of the surface. Floats within that meddy migrated to larger radius after the encounter, but the meddy survived with core tracer properties intact for another 1.5 years. Certainly, the survival of this meddy agrees with our expectations. The apparent radial displacement of the floats also has an analog with our experiments as the point vortices within the vortex were routinely shuffled during encounters. Apparently no floats have been observed to migrate inward, although such behavior does occur in our numerical model. This is problematic, although it might reflect sparsity of data.

Last, RT discuss Meddy 4 that was observed to change course from a dominantly westward path to a northwestward migration as it passed within 50 km of Santa Maria Island on its southwest side. It is tempting to ascribe this to near-field interactions between the meddy and its images, because our model predicts the seamount feedback on the meddy to be attractive for such locations.

In summary, observations of meddy–seamount interactions exhibit many of the characteristics found in our numerical model. Some of the comparisons, such as S95, suggest quantitative accuracy of the model. We thus now attempt to assess meddy–seamount impact on the Mediterranean salt tongue.

b. Salt tongue impact

The focal point of this analysis is the mean salinity equation (1). To facilitate comparisons with Armi and Stommel (1983), this equation is expressed in neutral coordinates (McDougall 1987), here denoted by γ. After averaging in time, (1) becomes

$$\overline{\mathbf{u}}\,\overline{z}_\gamma \cdot \boldsymbol{\nabla}_\gamma \overline{S} + \overline{u'z'_\gamma} \cdot \boldsymbol{\nabla}_\gamma \overline{S} + \overline{e}\overline{S}_\gamma = -\boldsymbol{\nabla}_\gamma \cdot (\overline{\mathbf{u}'S'}\overline{z}_\gamma + \overline{z'_\gamma S'}\overline{\mathbf{u}} + \overline{\mathbf{u}'z'_\gamma S'}) - (\overline{e'S'})_\gamma, \quad (7)$$

where overbars denote time mean and primes variations about that mean. The quantity z denotes a dependent variable describing the depth of the neutral surface γ, z_γ the ''thickness'' between two neutral surfaces and e dianeutral velocity. Equation (7) isolates all references to salinity anomalies on the right-hand side.

Over the meddy depth range, Armi and Stommel estimate

$$\overline{\mathbf{u}} \cdot \boldsymbol{\nabla}_\gamma \overline{S} = (-2 \pm 1) \times 10^{-10} \text{ psu s}^{-1} \quad (8)$$

using a velocity relative to 1000 dbar (which we accept here as absolute.) Clearly, (8) is related to the first quantity on the left of (7). But note the mean salinity structure requires balancing more than mean advection: eddy mass fluxes also can, through the second left-hand side quantity, affect the mean field. It is interesting to estimate if this is a large effect. From Armi and Stommel (1983), velocities at meddy depths are $\sim$0.0015 m s^{-1} toward the southwest. The net mass flux is thus

$$\int_{\gamma_b}^{\gamma_t} |\overline{\mathbf{u}}|\overline{z}_\gamma \, d\gamma \sim 0.0015 \text{ m s}^{-1} \, \delta z = 0.45 \text{ m}^2 \text{ s}^{-1},$$

assuming the 300-m thickness for this γ range suggested by the β-spiral data. We now estimate $\mathbf{u}'z'_\gamma$ considering the contribution from meddies. We assume 17 meddies per year of 30-km radius and 500-m height, the latter being a thickness anomaly of about 200 m. Hence meddies represent an anomalous eddy mass flux into the Mediterranean salt tongue area of

$$\frac{17 \text{ meddies}}{3 \times 10^7 \text{ s}} \pi (30 \text{ km})^2 200 \text{ m} \sim 0.3 \text{ Sv},$$

where Sv $\equiv 10^6$ m^3 s^{-1}.

The eastern edge of the β triangle is roughly 800 km, and, assuming all 17 meddies cross such a length, the meddy mass flux

$$\int_{\gamma_b}^{\gamma_t} |\overline{\mathbf{u}'z'_\gamma}| \, d\gamma \sim 0.4 \text{ m}^2 \text{ s}^{-1}$$

is comparable to mean flux. In addition, its direction is west-southwestward, like the mean flow. Since the mean salinity gradient is common to the mean and turbulent salt advection, meddy advective salt flux compares well to the mean flux. Thus, the Armi and Stommel estimate by itself might well underestimate the left-hand side of (7).

Of course, our estimate does not include nonmeddy effects. On the other hand, meddies are systematic in displacement and coherent; thus, they are plausibly the prevailing signal in regional eddy mass fluxes. In any case, we press on comparing our results with the Armi and Stommel estimate, while recalling the above point.

c. Quantitative comparison

Integrating (7) over the Mediterranean salt tongue yields

$$\iint \overline{\mathbf{u}}\,\overline{z}_\gamma \cdot \boldsymbol{\nabla}\overline{S} \, dA \sim -\iint [(\overline{e'S'})_\gamma + \overline{e}\overline{S}_\gamma] \, dA - \oint \overrightarrow{F(S')} \cdot \mathbf{n} \, dl, \quad (9)$$

where $\overrightarrow{F(S')}$ represents the eddy salinity anomaly fluxes. The input from meddies to the right-hand side is the residual of the salt anomaly flux in meddies crossing

the Mediterranean salt tongue boundaries. Assuming the Armi and Stommel estimate as representative of the Mediterranean salt tongue, (9) becomes

$$-2 \times 10^{-10} \text{ psu s}^{-1} \sim \overline{\mathbf{u}} \cdot \nabla \overline{S} \sim \frac{-\oint \overrightarrow{F(S')_{\text{MSI}}} \cdot \mathbf{n}\, dl}{A \overline{z}_\gamma} + \text{other}, \quad (10)$$

where A is the salt tongue area, the subscript ''MSI'' denotes flux discrepancies due to meddy–seamount interaction, ''other'' denotes nonmeddy–seamount interaction, and $\overline{z}_\gamma$ is the inverse of the regional stratification. This latter quantity needs to be compared with stratification anomalies appearing in $F(S')$ (i.e., the z'_γ quantities). Hydrography of the area (STR) shows the density range of a typical meddy, occupying 500 m in the vertical, will occupy 250 m in the background Atlantic. Hence, the total depth change in a meddy, expressed as the background depth change plus a perturbation depth change, implies that the ratio of z'_γ to $\overline{z}_\gamma$ is $O(1)$.

Substituting in numbers to (10) and denoting the salinity flux divergence due to meddy–seamount interaction by $-\nabla \cdot F_h$,

$$-\nabla \cdot \mathbf{F}_h \sim \frac{N\text{AR} \times \text{HR} \times \text{SA}(1 - \text{SR})}{\text{area}} = \frac{(17 \times 0.86) \times (\pi \times 30\,\text{km}^2) \times (1) \times (0.4) \times (0.3)}{17^\circ \times 17^\circ} = 0.4 \times 10^{-10}\,\text{psu s}^{-1}, \quad (11)$$

where N is the number of meddies interacting with seamounts per year, AR is a typical meddy area, HR is the ratio of meddy thickness anomaly to background thickness, SA is a typical meddy salt anomaly, and (1 − SR) is the meddy ''loss ratio'' (i.e., 1 − the survival ratio). The estimate, 0.4×10^{-10} psu s^{-1} is about 20% of the Armi and Stommel value. This is a lower bound because we used a survival rate of 0.7 (slightly larger than our average survival rate of 0.65) and a meddy salinity anomaly of 0.4 psu (the lower extreme of observed values). To estimate an upper bound we choose a salinity anomaly of 1.1 psu (an upper end for meddy salinity anomalies), decrease our survival rate to 0.6 (comparable to the smallest value in Table 1), and assume all meddies interact with topography. This increases the meddy–seamount flux estimate to

$$|\nabla \cdot \mathbf{F}_h| \sim \frac{N\text{AR} \times \text{HR} \times \text{SA}(1 - \text{SR})}{\text{area}} = \frac{(17 \times 1.0) \times (\pi \times 30\,\text{km}^2) \times (1) \times (1.1) \times (0.4)}{17^\circ \times 17^\circ} = 2.0 \times 10^{-10}\,\text{psu s}^{-1}, \quad (12)$$

that is, comparable to the Armi and Stommel estimate.

These numbers support the idea that meddy–seamount interaction is an important Mediterranean salt tongue maintenance mechanism. On the other hand, it appears not to be the only source. (Recall that the Armi Stommel number possibly underestimates advective salt flux divergence.) Meddy–seamount interaction might possibly provide 25%–50% of the needed salt supply. This study makes no statement about other sources, but possible candidates include mesoscale stirring into the background of Mediterranean undercurrent water and the interleaving-driven slow meddy decay described by Armi et al. (1989).

The above is an estimate of the global impact. We can also estimate local meddy impact by asking over what area the collision flux must be mixed to balance the Armi–Stommel advective flux estimate. The Horseshoe Seamounts interact with about 70% of the meddies (Richardson 2000). Therefore, the area over which the collision flux should be mixed is

$$\text{area} \sim \frac{N\text{AR} \times \text{HR} \times \text{SA}(1 - \text{SR})}{|\nabla \cdot \mathbf{F}_h|} = \frac{(17 \times 0.69) \times (\pi \times 30\,\text{km}^2) \times (1) \times (0.4) \times (0.3)}{2 \times 10^{-10}\,\text{psu s}^{-1}} \sim 10^\circ \times 10^\circ. \quad (13)$$

Local perturbations to the salt tongue appear near the Horseshoe Seamounts in Fig. 1. Given the above estimate, it is tempting to think some of the local anomalies are due to meddy–seamount interaction. On the other

hand, some of the structure appears west of the seamounts and so is not obviously related to them. Inferences must as yet be considered as speculative.

For the Great Meteor Seamounts, about 17% of the meddies interact with the seamounts (Richardson 2000). Thus,

$$\text{area} \sim \frac{N\text{AR} \times \text{HR} \times \text{SA}(1 - \text{SR})}{|\nabla \cdot \mathbf{F}_h|} = \frac{(17 \times 0.17) \times (\pi \times 30\ \text{km}^2) \times (1) \times (0.4) \times (0.3)}{2 \times 10^{-10}\ \text{psu s}^{-1}} \sim 5^\circ \times 5^\circ, \quad (14)$$

which is smaller than the area of Great Meteor Seamounts. Increasing the area to $10^\circ \times 10^\circ$ reduces the local effect to 25% of the advective flux. Thus it appears that near the Azores, meddy–seamount interaction is one of several salinity inputs. Note the mean salinity distribution in the area shows no smaller-scale structure.

5. Conclusions

Observations suggest that meddy–seamount interaction is an important mechanism for maintenance of Mediterranean salt tongue. If true, this challenges conventional diffusion models because it emphasizes the importance of both coherent vortex tracer transport and a specific coherent vortex dynamical mechanism. Neither effect is well modeled by down-mean-gradient transport, but such parameterizations are applied in nearly all numerical ocean simulations and in all current coupled climate models. In view of this, a three-layer, quasigeostrophic point vortex model was developed and applied to study meddy behavior near seamounts, with a view toward quantifying meddy–seamount impact on the Mediterranean salt tongue.

We have found meddies are surprisingly able to survive seamount encounters as coherent vortices. The reason for this is that meddies dynamically are strong potential vorticity anomalies, and it is difficult to destroy them. Even though they may be geometrically disrupted by topographic obstacles, the potential vorticity anomalies survive. Strong like-signed anomalies tend to reorganize and merge. Like-signed patches also have a tendency to resist distortion and therefore can hold themselves together when confronted with topographical-induced shearing stresses. Such dynamics have been recognized as central vortex processes for roughly 30 years (Christiansen and Zabusky 1973), suggesting their role will transcend our particular illustration.

We have attempted to estimate meddy–seamount interaction as an effect on the Mediterranean salt tongue. Two notable points emerge. First, meddy-driven mass flux appears to be significant in shaping mean salt tongue gradients. Second, our survival rates suggest meddy–seamount impact can provide one-quarter to one-half of the salinity flux divergence necessary to maintain the salt tongue. The balance of the needed rate (i.e., $\sim -1. \times 10^{-10}$ psu s^{-1}) potentially comes from other sources.

If our results are valid, meddy survival emerges as an important *limiting* factor on salt tongue amplitude because the meddies thus export salt away from the salt tongue anomaly. It is thus interesting to consider the consequences to a numerical model of an inaccurate mesoscale parameterization, such as if the meddies were all perfectly destroyed by seamounts. Then meddy–seamount flux divergence would grow to about $(-1.5$ to $-3.0) \times 10^{-10}$ psu s^{-1}. When combined with the above nonmeddy seamount background turbulent flux, the net forcing of the tongue would grow to $(-2.5$ to $-4.0) \times 10^{-10}$ psu s^{-1}. Something would need to change in the mean state to achieve a balance. An obvious possibility is the salt tongue would intensify, possibly by a factor of 2. A different possibility is that the mean flow could be affected, although the dynamical pathways by which this would occur are not obvious. In any case, changes in North Atlantic indices would result.

Currently, no coupled climate model performs at resolutions adequate to capture mesoscale ocean dynamics, much less submesoscale meddy–seamount interactions. Also, the tracer transport role of coherent vortices in eddy-resolving ocean-only simulations is unknown. Further, no coherent vortex parameterizations are currently used in any coupled climate or ocean-only model. Thus model physics maintaining numerical Mediterranean salt tongues are possibly distorted and, in a worst-case scenario, turbulent salinity flux are inaccurately estimated.

A summary message then of this work is that downgradient tracer diffusion parameterizations are indeed criticized, but not to the point of exclusion. A decidedly nonclassical salt transport mechanism, involving coherent vortex transport and their interaction with seamounts, does look like it is significant to the Mediterranean salt tongue. Getting the mesoscale dynamics of the seamount interaction ''right'' appears to be important. This can be parameterized in a noneddy-resolving model by the use of a modeler-specified survival ratio. Choosing a particular value should be done with care. Adopting our value of 0.65 now has some backing for modern climate simulations, but adhering to that value in climate change scenarios would be unwise. The best solution would be to directly compute vortex–seamount interaction, although current numerical methods for computing near strong topography are still problematic.

Acknowledgments. The authors gratefully acknowledge the support of the National Science Foundation through Grants ATM-9818628 and OCE-0220884 and NASA through NAG5-8291. Conversations with Michael Ghil and J. C. McWilliams were very helpful, and Ms. J. Jimeian is thanked for computational support.

APPENDIX

Vortex Counting Techniques

We have developed an automatic counting technique to quantify how many point vortices originally in the meddy end up in coherent structures. The goal of the procedure is to recognize sizeable numbers of coherently rotating point vortices within a deformation radius as coherent structures. The counting technique as used in applying this definition, however, is subject to some twists and turns that we now describe.

Our data consist of the locations of point vortices. For a given output field, for each point vortex, the number of neighboring point vortices lying within a circle of 30-km radius about it is determined. Thus, we obtain a vortex count for each point vortex. The two point vortices with the greatest counts and for which the groups composing their counts contained no common point vortices are then selected for further tests.

First, these collections were monitored to ensure their populations and counts were stable. In most cases, one of the groups was obviously bigger, and these always passed this temporal stability test. That collection was subsequently accepted as a postcollision coherent vortex. For the second core, a further criterion was applied: if the collection consisted of fewer than 20 vortices, it was discarded as representing a vortex that is too weak to survive. This criterion is somewhat arbitrary, but the reasoning behind it is that a vortex count of 20 within a 30-km radius circle represents a reduction in Rossby number from -0.2 to less than -0.04. Even though this Rossby number might be adequate to retain vortex coherence in our model, in the real ocean the competing effects of mesoscale shear and turbulence are likely to destroy it. If the point vortex count in the second collection was 30 or more, the second collection was counted as a coherent vortex. If the count was larger than 20, but less than 30, the effective radius of the collection was estimated using the average distance of the member point vortices from the core point vortex. If the radius was larger than 10 km, the second collection was counted as a coherent vortex.

The last criterion filtered small coherent structures that are likely to be eliminated by nonconservative processes and for which the quasigeostrophic approximation becomes somewhat suspicious. Last, we visually inspected the counts from several experiments and verified that the estimates generated by this procedure agreed with the counts that would have been assigned to the experiments if the estimation had been done by hand.

REFERENCES

Armi, L., and H. Stommel, 1983: Four views of a portion of the North Atlantic subtropical gyre. *J. Phys. Oceanogr.,* **13,** 828–857.

——, D. Hebert, N. Oakey, J. F. Price, P. Richardson, H. T. Rossby, and B. Ruddick, 1989: Two years in the life of a Mediterranean salt lens. *J. Phys. Oceanogr.,* **19,** 354–370.

Bower, A., L. Armi, and I. Ambar, 1997: Lagrangian observations of meddy formation during a Mediterranean undercurrent seeding experiment. *J. Phys. Oceanogr.,* **27,** 2545–2575.

Christiansen, J., and N. Zabusky, 1973: Instability, coalescence and fission of finite-area vortex structure. *J. Fluid Mech.,* **61,** 219–243.

Dewar, W., 2002: Baroclinic eddy interaction with isolated topography. *J. Phys. Oceanogr.,* **32,** 2789–2805.

Ebbesmeyer, C., B. A. Taft, and Coauthors, 1986: Detection, structure and origin of extreme anomalies in a Western Atlantic oceanographic section. *J. Phys. Oceanogr.,* **16,** 591–612.

Flierl, G., 1988: On the instability of geostrophic vortices. *J. Fluid Mech.,* **197,** 349–388.

Herbette, S., Y. Morel, and M. Arhan, 2003: Erosion of a surface vortex by a seamount. *J. Phys. Oceanogr.,* **33,** 1664–1679.

McDougall, T., 1987: Neutral surfaces. *J. Phys. Oceanogr.,* **17,** 2334–2342.

McDowell, S., and T. Rossby, 1978: Mediterranean water: An intense mesoscale eddy off the Bahamas. *Science,* **202,** 1085–1087.

McWilliams, J. C., 1985: Submesoscale coherent vortices in the ocean. *Rev. Geophys.,* **23,** 165–182.

Nof, D., 1981: On the β-induced movement of isolated, baroclinic eddies. *J. Phys. Oceanogr.,* **11,** 1662–1672.

Pierrehumbert, R., 1991: Chaotic mixing of tracer and vorticity by modulated traveling Rossby waves. *Geophys. Astrophys. Fluid Dyn.,* **58,** 285–319.

Prater, M., and T. Rossby, 1999: An alternative hypothesis for the origin of the ''Mediterranean'' salt lens observed off the Bahamas in the fall of 1976. *J. Phys. Oceanogr.,* **29,** 2103–2109.

Richardson, P. L., and A. Tychensky, 1998: Meddy trajectories in the Canary Basin measured during the SEMAPHORE experiment, 1993–1995. *J. Geophys. Res.,* **103,** 25 029–25 045.

——, D. Walsh, L. Armi, M. Schroder, and J. F. Price, 1989: Tracking three meddies with SOFAR floats. *J. Phys. Oceanogr.,* **19,** 371–383.

——, A. Bower, and W. Zenk, 2000: A census of meddies tracked by floats. *Progress in Oceanography,* Vol. 45, Pergamon, 209–250.

Schultz Tokos, K., and T. Rossby, 1991: Kinematics and dynamics of a Mediterranean salt lens. *J. Phys. Oceanogr.,* **21,** 879–892.

Shapiro, G. I., S. L. Meschanov, and M. V. Emelianov, 1995: Mediterranean lens ''Irving'' after its collision with seamounts. *Oceanol. Acta.,* **18,** 309–318.

Simmons, H., and D. Nof, 2000: Island as eddy splitters, I. *J. Mar. Res.,* **58,** 919–956.

Stern, M., 1999: Scattering of an eddy advected by a current towards a topographic obstacle. *J. Fluid. Mech.,* **402,** 211–223.

Wang, G., 2001: Meddy–seamount interaction: Implications for the Mediterranean Salt Tongue. M.S. thesis, Dept. of Oceanography, The Florida State University, 116 pp.